Quantum jump methods for the modelling of open quantum systems

Christopher Kitching

10134621

School of Physics and Astronomy

The University of Manchester

Fourth Year
MPhys Project

Jan 2021

This project was performed in collaboration with *Elanor Harrington*

Abstract

The aim of this project is to study open quantum systems: a quantum mechanical system which is in contact with environmental degrees of freedom. The study of such systems is crucial for real-world applications as no true quantum system is completely isolated from its surrounding. We look to outline the mathematical framework used to treat these systems with the main focus being to determine their time-evolution. This is done through solving effective equations of motion known as master equations. Particularly, we study a numerical technique called the quantum jump method which allows for calculation of the density matrix, an object containing all information about the system, as a stochastic average over many simulated trajectories of the systems wave-function with time. We will consider the numerical accuracy and physical interpretation of such a method and apply it in the case of both a simplified and more general spin-boson model.

1. Introduction

All physical quantum systems are comprised of both the system itself and its surrounding environment. Naturally, interactions occur which significantly change the dynamics of the system and lead to quantum dissipation, i.e information is lost to the environment. Thus, to obtain a complete understanding of real-world quantum systems, a different theoretical framework than that of unitary operators, used to treat closed systems, is required. Such work is crucial in many fields, for example in the development of future quantum technologies such as quantum computers where decoherence leads to errors in calculations.

Open quantum systems, by their very nature, cannot be in a pure state, i.e a state that completely determines the statistical outcome of a measurement. This motivated the formalism of an object known as the density matrix, an idea initially developed by John von Neumann in 1927 [1], which can describe any state, pure or mixed. The time evolution of such an object is governed by a master equation. In all but the most simple cases an analytical solution is not possible and even the numerical solutions are often particularly demanding [2, p; 60]. Instead, a method known as the quantum trajectory, or quantum jump, method can be used which reduces the complexity in exchange for introducing statistical averages.

We begin by introducing the mathematical formalism required for studying open-quantum systems. This includes a review of closed quantum systems, before introducing concepts such as the density matrix, interaction picture and ultimately a derivation of the Markovian master equation. The main focus of the paper begins in Section (3) where we introduce the numerical method of quantum trajectories, originally developed by Dalibard, Castin and Mølmer in the early 1990s [3]. How to apply such a method as a first-order Monte-Carlo algorithm is outlined and demonstrated to be mathematically equivalent to the master equation. The statistical errors involved for the method as well as its physical interpretations will be discussed. We then apply the technique to the case of a two-level system coupled to a bath of bosonic field modes, firstly to a simplified model and then the general case.

2. Theoretical background

Firstly, we look to develop the theoretical background necessary to understand the quantum trajectory method. We begin be reviewing closed quantum systems and then introduce tools such as the density operator and interaction picture, required to derive the master equation for open quantum systems.

2.1. Unitary time evolution of closed quantum systems

Note that throughout this report Plank's constant $\hbar$ will be set to one for simplicity. According to basic quantum mechanics, the state vector $|\psi(t)\rangle$, which mathematically describes the pure quantum state of an isolated quantum system, is described by a linear partial differential equation known as the Schrödinger equation [4, p; 1]

$$i\frac{d}{dt}|\psi(t)\rangle = H(t)\,|\psi(t)\rangle\,, \tag{2.1.1}$$

where $H(t)$ is the Hamiltonian of the system. Such an equation can be solved via means of the unitary time-evolution operator, $U(t, t_0)$, which transforms the initial state, $|\psi(t_0)\rangle$, at some initial time t_0, to a state at time t, $|\psi(t)\rangle$, [5, p; 145]

$$|\psi(t)\rangle = U(t, t_0) |\psi(t_0)\rangle . \tag{2.1.2}$$

For a closed system, the Hamiltonian is time-independent and thus equation (2.1.1) can be readily integrated to give

$$U(t, t_0) = e^{-iH(t-t_0)}. \tag{2.1.3}$$

From this expression it is clear that $U(t, t_0)$ satisfies the condition

$$U(t, t_0)U^\dagger(t, t_0) = U^\dagger(t, t_0)U(t, t_0) = I, \tag{2.1.4}$$

where I is the identity matrix, and hence $U(t, t_0)$ is a unitary operator.

In the situation of a time-dependent Hamiltonian, the solution to equation (2.1.1) can be written [6, p; 3]

$$U(t, t_0) = T_{\leftarrow}\exp\left[-i\int_{t_0}^{t} dsH(s)\right]. \tag{2.1.5}$$

$T_{\leftarrow}$ represents the chronological time ordering operator, which orders products of time-dependent operators such that their time-arguments increase in the direction of the arrow, right to left in this case.

2.2. The density operator

An alternative formalism to the language of state vectors is to use what is known as the density operator, or density matrix. This formulation is mathematically equivalent, and holds in the case of pure quantum states as above, but is particularly useful when dealing with mixed states, as any state can be represented by a single density matrix [7, p; 99].

The density operator for a system described by a pure state is defined by

$$\rho(t) \equiv |\psi(t)\rangle \langle\psi(t)| . \tag{2.2.1}$$

If instead the system is characterised by an ensemble of states, $\{|\psi_i(t)\rangle\}$, the density operator takes its most general form [8, p; 111]

$$\rho(t) \equiv \sum_i \rho_i |\psi_i(t)\rangle \langle\psi_i(t)| , \tag{2.2.2}$$

where ρ_i is the probability that the system realises the pure quantum state $|\psi_i(t)\rangle$. Using equation (2.1.2), this can be re-written as

$$\rho(t) = \sum_i \rho_i U(t, t_0) |\psi_i(t_0)\rangle \langle\psi_i(t_0)| U^\dagger(t, t_0) \tag{2.2.3}$$

$$= U(t, t_0)\left[\sum_i \rho_i |\psi_i(t_0)\rangle \langle\psi_i(t_0)|\right] U^\dagger(t, t_0), \tag{2.2.4}$$

and thus the density operator evolves in time according to the unitary transformation

$$\rho(t) = U(t, t_0)\rho(t_0)U^\dagger(t, t_0). \tag{2.2.5}$$

Differentiating equation (2.2.5) with respect to time, we obtain an equation of motion for the density operator,

$$\frac{\partial}{\partial t}\rho = -i[H(t), \rho(t)], \tag{2.2.6}$$

which is known as the Liouville-von Neumann equation [8, p; 111] and governs the evolution of both pure and mixed state density operators for closed systems.

The density operator has several useful properties that we will exploit throughout this report. Firstly, it is a Hermitian operator, which can be readily seen from equation (2.2.2). It can also be easily shown that the expectation of any general operator, $\hat{O}$, is given by taking the trace of $\hat{O}\rho$, [6, p; 11]

$$\left\langle \hat{O} \right\rangle \equiv Tr\left(\hat{O}\rho\right) = Tr\left(\hat{O}\sum_i |\psi_i\rangle \langle\psi_i|\right) \tag{2.2.7}$$

$$= \sum_n \sum_i \langle n|\hat{O}|\psi_i\rangle \langle\psi_i|n\rangle = \sum_i \langle\psi_i| \left(\sum_n |n\rangle \langle n|\right) \hat{O} |\psi_i\rangle \tag{2.2.8}$$

$$= \sum_i \langle\psi_i|\hat{O}|\psi_i\rangle, \tag{2.2.9}$$

which is the definition of the expectation of an operator $\hat{O}$.

2.3. The interaction picture

In the above formalism of the density operator we have worked in what is known as the Schrödinger picture, where we allow the state vectors to evolve with time but the operators are held constant with respect to time. The opposite formalism, where the operators incorporate a time-dependency but the states are time independent, is called the Heisenberg picture [9, pp; 80-81]. There exists an intermediate representation of these two pictures, known as the interaction or Dirac picture, which we will make frequent use of in our derivations of master equations.

To see why this is a useful tool, consider the partitioning of the full Hamiltonian, H,

$$H = H_0 + H_I, \tag{2.3.1}$$

where H_0 is generally chosen to be simple and exactly soluble, while H_I contains more complex, perturbative terms. Note that H is taken to be time-independent for simplicity, but in general could contain explicit time dependence, for example if the quantum system interacts with a time-varying electric field. In such a case, we include the explicitly time-dependent terms in H_I.

In order for the interaction picture to be physically viable we require that the expectation of operators remains unchanged when changing pictures. Using equations (2.2.5) and (2.2.7) we first write

$$\left\langle \hat{O}(t) \right\rangle = Tr\left(\hat{O}\rho(t)\right) = Tr\left(\hat{O}U(t, t_0)\rho(t_0)U^\dagger(t, t_0)\right), \tag{2.3.2}$$

and then split the time-evolution operator as

$$U(t,t_0) \equiv U_0(t,t_0)U_I(t,t_0), \tag{2.3.3}$$

where these time-evolution operators are defined analogously to that of equation (2.1.3). Substituting equation (2.3.3) into equation (2.3.2) gives

$$\left\langle \hat{O} \right\rangle = Tr\left(\hat{O}U_0(t,t_0)U_I(t,t_0)\rho(t_0)U_I^\dagger(t,t_0)U_0^\dagger(t,t_0)\right). \tag{2.3.4}$$

Using the following cyclic trace property [10]

$$Tr(ABC) = Tr(CAB) = Tr(BCA), \tag{2.3.5}$$

this can be re-written as

$$\left\langle \hat{O} \right\rangle = Tr\left(U_0^\dagger(t,t_0)\hat{O}U_0(t,t_0)U_I(t,t_0)\rho(t_0)U_I^\dagger(t,t_0)\right) \tag{2.3.6}$$

$$\equiv Tr\left(\hat{\tilde{O}}\tilde{\rho}(t)\right), \tag{2.3.7}$$

where we have defined

$$\hat{\tilde{O}}(t) \equiv U_0^\dagger(t,t_0)\hat{O}U_0(t,t_0), \tag{2.3.8}$$

$$\tilde{\rho}(t) \equiv U_I(t,t_0)\rho(t_0)U_I^\dagger(t,t_0), \tag{2.3.9}$$

$$= U_0^\dagger(t,t_0)\rho(t)U_0(t,t_0), \tag{2.3.10}$$

which are rules for transforming our operators to the interaction picture. We now see why the interaction picture is useful. Effectively, we have absorbed the easily solvable part of the Hamiltonian, H_0, into the definitions of the states and operators. Thus, all of the dynamics in this picture are associated with the more complicated interaction part, H_I, which we will treat as a perturbation.

As in equation (2.2.6), the interaction picture density evolution has Liouville-von Neumann form

$$\frac{\partial\tilde{\rho}(t)}{\partial t} = -i[\tilde{H}(t),\tilde{\rho}(t)]. \tag{2.3.11}$$

Again, with analogy to equation (2.1.5), if the Hamiltonian has time-dependence the unitary operator can instead be written

$$U_I(t,t_0) = T_{\leftarrow}\exp\left[-i\int_{t_0}^{t} ds\tilde{H}(s)\right]. \tag{2.3.12}$$

2.4. Open quantum systems

Having now studied closed quantum systems, along with the generalisation to mixed states through the density operator and introduction of the interaction picture to simplify the problem, we turn to open quantum systems. We will introduce the general framework and then derive the Markovian master equation before considering some specific examples.

2.4.1 General framework

In the case of open quantum systems, we consider a system, S, coupled to a large environment, E. In this setup, we partition the Hamiltonian in the following way

$$H = H_S + H_E + H_I, \tag{2.4.1}$$

where H_S and H_E are the contributions of the system and environment respectively, and describe the coherent dynamics of their relative degrees of freedom. The interaction between the system and the reservoir is detailed in H_I. Figure 1 illustrates this idea schematically.

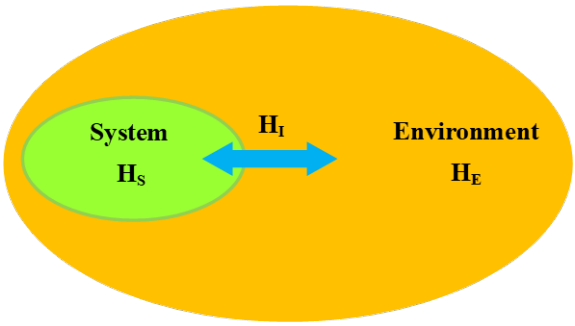

Figure 1: Image showing the the general framework of an open quantum system. The open system, S, is the subsystem of a larger combined system, $S+E$, where E represents the environment. The dynamics of the system and environment degrees of freedom are described by their respective Hamiltonian's, H_S and H_E, with H_I describing the interaction between the two. This image was created using tools in Microsoft Publisher.

In what follows we will use what is known as the reduced density operator

$$\rho_s(t) = Tr_E(\rho(t)), \tag{2.4.2}$$

where we have used the partial trace operation to "trace out" the environmental degrees of freedom. This is useful as ρ_S has dimensions much less than the full density operator while maintaining all information about the system, S. To see this, note that the system and environment are separate Hilbert spaces, thus any observable of our system can be written as a tensor product

$$\hat{O} = \hat{O}_S \otimes \mathbb{1}_E, \tag{2.4.3}$$

where $\mathbb{1}_E$ is the identity. Then using (2.3.2) we can write

$$\left\langle \hat{O} \right\rangle = Tr_{S+E}(\hat{O}_S \otimes \mathbb{1}_E \rho(t)) = Tr(\hat{O}_S \rho_S(t)), \tag{2.4.4}$$

i.e $\left\langle \hat{O} \right\rangle$ is fully described by $\rho_S(t)$.

2.4.2 Markovian master equations

Knowing that $\rho_S(t)$ is the object we wish to work with, we seek an equation that governs its dynamical evolution in order to determine the system behaviour under the influence of the environment.

We begin by treating the H_I term in equation (2.4.1) as a small perturbation and make the connection with equation (2.3.1) to identify $H_0 = H_S + H_E$. Equation (2.3.11) can be solved to give

$$\tilde{\rho}(t) = \rho(0) - i \int_0^t ds[\tilde{H}_I(s), \tilde{\rho}(s)], \tag{2.4.5}$$

and then substituting this back into equation (2.3.11) gives

$$\frac{\partial \tilde{\rho}(t)}{\partial t} = -i[\tilde{H}_I(t), \tilde{\rho}(0)] - \int_0^t ds \left[\tilde{H}_I(t), [\tilde{H}_I(s), \tilde{\rho}(s)]\right]. \tag{2.4.6}$$

Finally, as noted in Sub-section (2.4.1), we take the partial trace over the environment to give

$$\frac{\partial \tilde{\rho}_S(t)}{\partial t} = -iTr_E[\tilde{H}_I(t), \tilde{\rho}(0)] - \int_0^t ds \, \mathrm{Tr}_E \left[\tilde{H}_I(t), [\tilde{H}_I(s), \tilde{\rho}(s)]\right]. \tag{2.4.7}$$

Of course, this equation is still exact, but we can make a number of simplifying assumptions [11, pp; 12-13]:

1. Firstly, at the initial time $t = 0$, we assume that the system and environment can be separated as $\rho(0) = \rho_S(0) \otimes \rho_E(0)$, i.e there are no correlations between the system and the bath.

2. We assume the environment to be thermal such that [11, p; 13]

$$\rho_E = \frac{\exp\left(\frac{H_E}{k_B T}\right)}{\mathrm{Tr}\left(\exp\left(\frac{H_E}{k_B T}\right)\right)}. \tag{2.4.8}$$

   In the case, with linear bosonic operators, the first term can then be shown to be zero.

3. The Born approximation extends assumption 1 to all times, $\tilde{\rho}(t) \approx \tilde{\rho}(t) \otimes \rho_E(0)$. Due to the interaction Hamiltonian, some correlations are expected to appear. However, given that we are in the weak coupling regime, and that the environment is large relative to the system, so it is essentially unaffected by coupling to the system, this approximation is valid.

4. The Markov approximation allows us to replace $\rho_I(t)$ with $\rho_I(s)$, i.e we remove the density operator's dependence on its past to make the equation memoryless. So long as the correlation (memory) time of the environment, i.e. the time over which the environment preserves information about past system states, is much smaller than the typical time scale for system evolution, this is a justified assumption. There remains a dependence on the initial state preparation of the system, but this can be removed via the substitution $s \longrightarrow t - s$ and then extending the upper limit of integration to infinity without changing the outcome by means of our previous discussion of timescales.

Through these four approximations, equation (2.4.7) can be written in the form

$$\frac{\partial \tilde{\rho}_S(t)}{\partial t} = -\int_0^\infty ds Tr_E \left[\tilde{H}_I(t), [\tilde{H}_I(t-s), \tilde{\rho}_S(t) \otimes \rho_E]\right], \tag{2.4.9}$$

which is known as the weak-coupling Markovian master equation in the interaction picture.

Consider now an interaction Hamiltonian of the form [11, p; 14]

$$H_I = \sum_\alpha A_\alpha \otimes B_\alpha, \tag{2.4.10}$$

where A_α and B_α are the system and environment operators respectively. Again, using equation (2.3.8) we transform to the interaction picture

$$\tilde{H}_I(t) = \sum_\alpha A_\alpha(t) \otimes B_\alpha(t), \tag{2.4.11}$$

where $A_\alpha(t) = e^{iH_S t} A_\alpha e^{-iH_S t}$ and $B_\alpha(t) = e^{iH_E t} B_\alpha e^{-iH_E t}$. We also introduce environment correlation functions [6, p; 31]

$$C_{\alpha\beta} = \left\langle B_\alpha(t) B_\beta(s) \right\rangle_E = Tr(B_\alpha(t) B_\beta(s) \rho_E), \tag{2.4.12}$$

where we have again used equation (2.2.7) to write the expectation as a trace. In the case of a stationary environment, i.e $[H_E, \rho_E] = 0$, it can easily be shown, with use of the cyclic trace property stated in equation (2.3.5), that

$$C_{\alpha\beta} = Tr_E(B_\alpha(t-s) B_\beta \rho_E) \equiv C_{\alpha\beta}(t-s). \tag{2.4.13}$$

Now, expanding out the commutators in the master equation (2.4.9), substituting in the expression for the decomposed Hamiltonian, $\tilde{H}_I$, as stated in equation (2.4.11), and using the environment correlation functions in equation (2.4.13), we get

$$\frac{\partial \tilde{\rho}_S(t)}{\partial t} = -\sum_{\alpha\beta} \int_0^\infty d\tau \left([A_\alpha(t), A_\beta(t-\tau)\tilde{\rho}(t)] C_{\alpha\beta} + [\tilde{\rho}_S(t) A_\beta(t-\tau), A_\alpha(t)] C_{\beta\alpha}(-\tau) \right), \tag{2.4.14}$$

where we have dropped the tensor direct products to lighten the notation.

To transform this equation back to the Schrödinger picture we first note that, using equation (2.3.8), the density matrix for our system in the interaction picture is

$$\tilde{\rho}_S(t) = e^{iH_S t} \rho_S(t) e^{-iH_S t}. \tag{2.4.15}$$

Rearranging this equation and then differentiating with respect to time we get a transformation from the interaction picture to Schödinger picture for the evolution of the system density matrix

$$\frac{\partial \rho_S(t)}{\partial t} = -i[H_S, \rho_S(t)] + e^{-iH_S t} \left(\frac{\partial \tilde{\rho}_S(t)}{\partial t} \right) e^{iH_S t}. \tag{2.4.16}$$

Finally, we use this equation to transform equation (2.4.14) back to the Schödinger picture which gives what is known as the Schödinger picture master equation

$$\begin{aligned} \frac{\partial \rho_S(t)}{\partial t} = -i[H_S, \rho_S(t)] - \sum_{\alpha\beta} \int_0^\infty d\tau \Big(& [A_\alpha, A_\beta(-\tau)\rho_S(t)] C_{\alpha\beta}(\tau) \\ & + [\rho_S(t) A_\beta(-\tau), A_\alpha] C_{\beta\alpha}(-\tau). \end{aligned} \tag{2.4.17}$$

The first term on the left hand side generates unitary evolution due to H_S while the remaining terms describe the influence on the environment leading to dissipation for example.

2.4.3 Illustrative example: spin-boson model

Although trajectory methods are the main focus of this report, it is useful to exactly solve the master equation as a comparison. To take the Schrödinger picture Born-Markov master equation further we require specific models, unfortunately very few are exactly solvable. Ultimately, we seek to derive equations of Lindbladian form, the most general type of Markovian master equation [11], which can then be readily solved. We shall consider the example of a two-level system coupled to a bath of harmonic oscillators, firstly for the simplified case and then more generally.

2.4.3.1 Simplified model without tunnelling

In this first simplified case, we consider the spin-boson model where we ignore the tunnelling term so the occupation of each level of the system would be conserved if the system were closed. Physically this could represent for example a two-level atom interacting with an electromagnetic field.

We consider partitioning the Hamiltonian as in equation (2.4.1) where the system Hamiltonian is taken to be

$$H_S = \frac{\epsilon}{2}\sigma_z = \frac{\epsilon}{2}\left(|e\rangle\langle e| - |g\rangle\langle g|\right), \tag{2.4.18}$$

where ϵ is the energy splitting between the excited state, $|e\rangle$, and ground state, $|g\rangle$, of the system. We are not driving the system here, so there are no transitions between states. The environment Hamiltonian is give by

$$H_E = \sum_{\mathbf{k}} \omega_{\mathbf{k}} b^\dagger_{\mathbf{k}} b_{\mathbf{k}}, \tag{2.4.19}$$

which is essentially a bath of harmonic oscillators (bosons) of frequency $\omega_{\mathbf{k}}$, with creation and annihilation operators $b^\dagger_{\mathbf{k}}$ and $b_{\mathbf{k}}$. Finally the interaction Hamiltonian is

$$H_I = \sum_{\mathbf{k}} (g_{\mathbf{k}}\sigma_+ b_{\mathbf{k}} + g^*_{\mathbf{k}}\sigma_- b^\dagger_{\mathbf{k}}), \tag{2.4.20}$$

where $g_{\mathbf{k}}$ and $g^*_{\mathbf{k}}$ are coupling constants.

The details of the derivation are omitted as our main focus is on the trajectory method, this solution is only used for comparison. However, the general idea would be to expand the commutators and evaluate the correlation functions of equation (2.4.17), subject to the Hamiltonian's written above. Ultimately, the final result, which is known as the optical master equation, is

$$\begin{aligned}\frac{\partial \rho_S}{\partial t} =& -i\frac{\epsilon'}{2}[\sigma_z, \rho_S] \\ &+ \Gamma(\epsilon)(N(\epsilon)+1)(2\sigma_-\rho_S\sigma_+ - \{\sigma_+\sigma_-, \rho_S\}) \\ &+ \Gamma(\epsilon)N(\epsilon)(2\sigma_+\rho_S\sigma_- - \{\sigma_-\sigma_+, \rho_S\}),\end{aligned} \tag{2.4.21}$$

where ϵ' is just a shifted energy scale known as the Lamb shift which is generally considered negligible. The square bracers are commutators and the curly bracers are anti-commutators. $N(\epsilon)$ is the Bose-Einstein occupation number defined by [6, p; 2]

$$N(\epsilon) = \left(e^{\frac{\epsilon}{k_B T}} - 1\right)^{-1}, \tag{2.4.22}$$

where T is the bath temperature and k_B is the Boltzmann constant. $\Gamma(\epsilon)$ are rates, in this case defined to be $\Gamma(\epsilon) = \pi J(\epsilon)$, where $J(\epsilon)$ is the spectral density defined by [12, p; 7]

$$J(\epsilon) = \sum_{\mathbf{k}} |g_{\mathbf{k}}|^2 \delta(\epsilon - \epsilon_{\mathbf{k}}), \tag{2.4.23}$$

which describes the density of the bath modes weighted by the square of their individual coupling strength to the system.

The first term of equation (2.4.21) describes coherent system dynamics, the second term describes decay due to both spontaneous and stimulated emission, at rates proportional to $\Gamma(\epsilon)$ and $\Gamma(\epsilon)N(\epsilon)$ respectively, and the third term describes absorption at a rate proportional to $\Gamma(\epsilon)N(\epsilon)$.

This can be seen more clearly if we write out two of the differential equations of equation (2.4.21) explicitly as

$$\dot{\rho}_{ee}(t) = -2\Gamma(N+1)\rho_{ee}(t) + 2\Gamma N \rho_{gg}(t), \tag{2.4.24}$$

$$\dot{\rho}_{gg}(t) = -2\Gamma N \rho_{gg}(t) + 2\Gamma(N+1)\rho_{ee}(t), \tag{2.4.25}$$

where, to lighten notation, $\Gamma \equiv \Gamma(\epsilon)$ and $N \equiv N(\epsilon)$. These equations are Einstein rate equations [13, p; 3], thus demonstrating explicitly the physical interpretation of the coefficients as rates.

We can extend the no tunnelling model slightly by adding a driving term to the system Hamiltonian so that it reads

$$H_S = \frac{\epsilon}{2}\sigma_z + \Omega \cos(\omega_l t)\sigma_x, \tag{2.4.26}$$

where ω_l is the driving frequency and Ω is known as the Rabi frequency, which is proportional to the interaction strength between the light and atomic transition, and the amplitude of the lights electric field [14]. To clarify, we are driving a two-level system with atomic transition frequency ϵ, with light of frequency ω_l. The system thus absorbs photons and then re-emits them via stimulated emission and thus the state oscillates at the Rabi frequency Ω. In this case, we move to a rotating frame and use the rotating-wave (secular) approximation, allowing us to ignore fast-oscillating terms and thus remove the time-dependence from our Hamiltonian [15]. Such an approximation is only valid if $\epsilon \gg \Omega$, which is often the case. This leads to the optical master equation for a driven system in the rotating frame,

$$\begin{aligned}\frac{\partial \rho_S'}{\partial t} =& -i\frac{\nu'}{2}[\sigma_z, \rho_S'] - i\frac{\Omega}{2}[\sigma_x, \rho_S'] \\ &+ \Gamma(\epsilon)(N(\epsilon)+1)(2\sigma_- \rho_S \sigma_+ - \{\sigma_+\sigma_-, \rho_S'\}) \\ &+ \Gamma(\epsilon)N(\epsilon)(2\sigma_+ \rho_S \sigma_- - \{\sigma_-\sigma_+, \rho_S'\}),\end{aligned} \tag{2.4.27}$$

where the ' notation indicates we are in the rotating frame and ν is the detuning of the driving frequency from resonance, $\nu = \epsilon - \omega_l$ [16, p; 104]. Again, this shift term is often ignored.

It is possible to cast equation (2.4.27) as the following matrix equation

$$\frac{d}{dt}\begin{pmatrix}\rho_{ee}' \\ \rho_{ge}' \\ \rho_{eg}' \\ \rho_{gg}'\end{pmatrix} = \begin{pmatrix} -2\Gamma(\epsilon)(1+N(\epsilon)) & i\frac{\Omega}{2} & -i\frac{\Omega}{2} & 2\Gamma(\epsilon)N(\epsilon) \\ i\frac{\Omega}{2} & -i\nu' - \Gamma(\epsilon)(2N(\epsilon)+1) & 0 & -i\frac{\Omega}{2} \\ -i\frac{\Omega}{2} & i\frac{\Omega}{2} & i\nu' - \Gamma(\epsilon)(2N(\epsilon)+1) & 0 \\ 2\Gamma(\epsilon)(N(\epsilon)+1) & -i\frac{\Omega}{2} & i\frac{\Omega}{2} & -2\Gamma(\epsilon)N(\epsilon) \end{pmatrix}\begin{pmatrix}\rho_{ee}' \\ \rho_{ge}' \\ \rho_{eg}' \\ \rho_{gg}'\end{pmatrix}. \tag{2.4.28}$$

This matrix equation can then be solved exactly, although the solution is complicated. We only seek the steady-state low temperature solution for comparison purposes, in which case the solution for the excited state population reduces to [17, p; 96]

$$\rho_{ee} = \frac{\frac{1}{4}|\Omega|^2}{\Delta^2 + \frac{1}{4}\Gamma^2 + \frac{1}{2}|\Omega|^2}. \tag{2.4.29}$$

2.4.3.2 General model with tunnelling

We now look to generalise the above model by adding in a tunnelling term, which could for example correspond to population oscillations between states of two different wells in a double well potential setup. The total Hamiltonian now reads [18, p; 3]

$$H_{\text{tot}} = \frac{\nu}{2}\sigma_z + \frac{\Delta}{2}\sigma_x + \sum_{\mathbf{k}} \omega_{\mathbf{k}} b^\dagger_{\mathbf{k}} b_{\mathbf{k}} + \sigma_z \sum_{\mathbf{k}} g_{\mathbf{k}}(b^\dagger_{\mathbf{k}} + b_{\mathbf{k}}), \tag{2.4.30}$$

where Δ is the tunnelling matrix element.

We switch to the eigenbasis of H_S for convenience, which can be shown to be

$$|+\rangle = \sin\left(\frac{\theta}{2}\right)|g\rangle + \cos\left(\frac{\theta}{2}\right)|e\rangle, \tag{2.4.31}$$

$$|-\rangle = \cos\left(\frac{\theta}{2}\right)|g\rangle - \sin\left(\frac{\theta}{2}\right)|e\rangle, \tag{2.4.32}$$

where $|g\rangle$ and $|e\rangle$ are the z-basis eigenvectors we have previously been using and $\theta = \tan^{-1}\left(\frac{\Delta}{\epsilon}\right)$.

Again, we omit the derivation, but essentially we evaluate the commutators and correlation functions of equation (2.4.17) to get the master equation in Lindblad form

$$\begin{aligned}\frac{\partial\rho(t)}{\partial t} = -i[H_s + H_{LS}, \rho_S(t)] &+ \Gamma_0\left(P_0\rho_S(t)P_0 - \frac{1}{2}\{P_0^2, \rho_S(t)\}\right) \\ &+ \Gamma(\eta)(1+N(\eta))\left[P_\eta\rho_S(t)P_\eta^\dagger - \frac{1}{2}\{P_\eta^\dagger P_\eta, \rho_S(t)\}\right] \\ &+ \Gamma(\eta)N(\eta)\left[P_\eta^\dagger\rho_S(t)P_\eta - \frac{1}{2}\{P_\eta P_\eta^\dagger, \rho_S(t)\}\right],\end{aligned} \tag{2.4.33}$$

where $\eta = \sqrt{\nu^2 + \Delta^2}$. P_0 and P_η are operators defined in the following manner

$$P_0 = \frac{\epsilon}{\eta}\left(|+\rangle\langle+| - |-\rangle\langle-|\right), \tag{2.4.34}$$

$$P_\eta = \frac{\Delta}{\eta}|-\rangle\langle+|, \tag{2.4.35}$$

where we see that P_η changes the state entirely whereas P_0 is simply a phase change. Γ_0 and $\Gamma(\eta)$ are the rates defined as

$$\Gamma_0 = 2\pi \lim_{\epsilon\to 0} J(\epsilon)(1+N(\epsilon)), \tag{2.4.36}$$

$$\Gamma(\eta) = 2\pi J(\eta). \tag{2.4.37}$$

Note, that again we have employed the rotating wave approximation to remove fast-oscillating terms. This leads to a condition of the form $\eta \gg \Gamma$, similar to before.

Analogously to the case without tunnelling, equation (2.4.27), the first term of equation (2.4.33) is a combination of the system and Lamb-shift Hamiltonian's, the later often being negligible, which give rise to coherent dynamics. The remaining terms cause dissipation and decoherence at their respective rates.

3. Quantum trajectories

Quantum trajectory techniques originated in quantum optics and provide a method of numerically solving dissipate dynamics for a system where the density operator is described by a master equation in Lindblad form [19]. The method involves re-writing the master equation as a stochastic average over individual trajectories, which are evolved in time using a numerical technique such as the Monte Carlo method. This has advantages over the alternative of propagating the full density matrix. Most notably, if the space you are working in has dimension N then evolving the full matrix requires evolving an object of size N^2, whereas the quantum trajectory method requires propagation of the state vectors, which are only of size N. Additionally, the method provides some intuitive insight into what is physically happening, better allowing us to interpret the dynamics. The main drawback is the need to average over multiple samples, however this process can be parallelised to make it more efficient.

In Sub-section (2.4.3) we derived equations of Lindblad form for two specific cases, namely equations (2.4.27) and (2.4.33), but in general the Markovian master equation, working in natural units with $\hbar = 1$, has a Lindblad form [8]

$$\frac{\partial \rho_S(t)}{\partial t} = -i[H(t), \rho_S(t)] - \frac{1}{2}\sum_m \Gamma_m (c_m^\dagger c_m \rho_S(t) + \rho_S(t) c_m^\dagger - 2 c_m \rho_S(t) c_m^\dagger), \tag{3.0.1}$$

where c_m are the Lindblad operators, or jump operators, that describe dissipative dynamics that occur at characteristic rates Γ_m. Equation (3.0.1) can be re-written in the form [17, p; 86]

$$\frac{\partial \rho_S(t)}{\partial t} = -i(H_{\text{eff}} \rho_S(t) - \rho_S(t) H_{\text{eff}}^\dagger) + \sum_m \Gamma_m c_m \rho_S(t) c_m^\dagger, \tag{3.0.2}$$

where the effective Hamiltonian, H_{eff}, is defined as [17, p; 86]

$$H_{\text{eff}} = H_S - \frac{i}{2}\sum_m \Gamma_m c_m^\dagger c_m. \tag{3.0.3}$$

It is this non-Hermitian effective Hamiltonian that we are interested in with regards to quantum trajectories.

3.1. Stochastic averages and quantum mechanical expectation values

An important distinction needs to be made between the statistical average and the quantum mechanical expectation value of an operator $\hat{A}$. The expectation of an operator can be determined

using the density matrix, ρ, as in equation (2.2.7). If the density matrix can be expanded in terms of pure states, as in equation (2.2.1), then the expectation of $\hat{A}$ can be expanded as

$$\langle A \rangle = Tr(A\rho) = \sum_i p_i \langle \phi_i | A | \phi_i \rangle \equiv \sum_i p_i A_i \equiv \bar{A}, \tag{3.1.1}$$

where $\langle \phi_i | A | \phi_i \rangle$ is the quantum mechanical expectation value and the weighted sum of said value gives the statistical average. In what follows we denote the total expectation of $\hat{A}$ using angled bracers, $\langle A \rangle$, and the statistical average with an over-line, $\bar{A}$.

3.2. First-order Monte Carlo wavefunction method

For simplicity, we will use a method that is first-order in the time-step, δt, but a higher order method is outlined in Sub-section (3.5). The algorithm proceeds as follows [17, pp; 88-89]:

1. Choose an initial state, $|\psi(t=0)\rangle$.

2. Take the initial state and propagate it under the effective Hamiltonian to find a candidate state at time $t + \delta t$,

$$\left|\psi^{(1)}(t+\delta t)\right\rangle = e^{-iH_{\text{eff}}\delta t} |\psi(t)\rangle \approx (1 - iH_{\text{eff}}\delta t) |\psi(t)\rangle . \tag{3.2.1}$$

3. Compute the norm of the candidate state,

$$\left\langle \psi^{(1)}(t+\delta t) \middle| \psi^{(1)}(t+\delta t) \right\rangle = \langle \psi(t)| (1 + iH^{\dagger}_{\text{eff}}\delta t)(1 - iH_{\text{eff}}\delta t) |\psi(t)\rangle \tag{3.2.2}$$

$$\approx 1 - \delta t \langle \psi(t)| i(H_{\text{eff}} - H^{\dagger}_{\text{eff}}) |\psi(t)\rangle \tag{3.2.3}$$

$$\equiv 1 - \delta p. \tag{3.2.4}$$

   Note that δp can arise from the action of different Lindblad operators, c_m,

$$\delta p = \delta t \sum_m \langle \psi(t)| c^{\dagger}_m c_m |\psi(t)\rangle \tag{3.2.5}$$

$$\equiv \sum_m \delta p_m, \tag{3.2.6}$$

   where δp_m is the probability that the operator c_m will act in this time-step.

4. Draw a random number, r_1, between 0 and 1 from a uniform distribution. Then propagate the state statistically in the following way:

   (a) If $r_1 > \delta p$, no jump occurs, and we propagate the state under H_{eff},

$$|\psi(t+\delta t)\rangle = \frac{\left|\psi^{(1)}(t+\delta t)\right\rangle}{\sqrt{1-\delta p}}. \tag{3.2.7}$$

   This 'no jump' situation occurs with probability $1 - \delta p$.

(b) If $r_1 < \delta p$, a jump occurs, and we choose the particular jump operator to apply by means of the following:

i. Associate each m with an interval of size proportional to δp_m, normalised to total length one so that each m uniquely corresponds to a range between 0 and 1.

ii. Draw a second random number, r_2, again uniformly distributed between 0 and 1.

iii. Choose the associated c_m for which its assigned interval contains r_2. The probability to choose such an operator would be

$$\Pi_m = \frac{\delta p_m}{\delta p}. \tag{3.2.8}$$

iv. Apply the chosen operator to propagate the state as

$$|\psi(t+\delta t)\rangle = \frac{c_m |\psi(t)\rangle}{\sqrt{\frac{\delta p_m}{\delta t}}}. \tag{3.2.9}$$

This 'jump' situation occurs with total probability δp.

It is easy to show that this method is equivalent to the master equation as written in equation (3.0.2). First we define the density operator in the usual manner,

$$\sigma(t) = |\phi(t)\rangle \langle\phi(t)| . \tag{3.2.10}$$

Then using equations (3.2.7) and (3.2.9) the statistical average of the density operator is

$$\overline{\sigma(t+\delta t)} = (1-\delta p)\frac{\left|\phi^{(1)}(t+\delta t)\right\rangle}{\sqrt{1-\delta p}}\frac{\left\langle\phi^{(1)}(t+\delta t)\right|}{\sqrt{1-\delta p}} + \delta p \sum_m \Pi_m \frac{c_m |\phi(t)\rangle}{\sqrt{\frac{\delta p_m}{\delta t}}}\frac{\langle\phi(t)| c_m^\dagger}{\sqrt{\frac{\delta p_m}{\delta t}}}, \tag{3.2.11}$$

where we have used the notation convention outlined in Sub-section (3.1). Using the definitions in equations (3.2.1), (3.2.8) and (3.2.10) we obtain

$$\overline{\sigma(t+\delta t)} = \sigma(t) - i\delta t(H_{\text{eff}}\sigma(t) - \sigma(t)H_{\text{eff}}^\dagger) + \delta t \sum_m c_m \sigma(t) c_m^\dagger, \tag{3.2.12}$$

which holds regardless of whether $\sigma(t)$ is comprised of pure or mixed states. Rearranging slightly and taking the $\delta t \to 0$ limit leads to

$$\dot{\sigma}(t) = \lim_{\delta t \to 0}\left(\frac{\overline{\sigma(t+\delta t)} - \sigma(t)}{\delta t}\right) \tag{3.2.13}$$

$$= -i(H_{\text{eff}}\sigma(t) - \sigma(t)H_{\text{eff}}^\dagger) + \sum_m c_m \sigma(t) c_m^\dagger, \tag{3.2.14}$$

which is identical to equation (3.0.2) demonstrating that taking a stochastic average over trajectories is equivalent to the master equation.

3.3. Statistical errors

From the discussion of the first-order quantum trajectories method, the natural question that arises is how many trajectories, N, are required for good convergence. Assuming that our random numbers are truly random, all the trajectories will be statistically independent. Hence, employing concepts like central limit theorem, it can be shown that the statistical error, σ_A, in the value we are attempting to estimate, A, is given by [17, p; 91]

$$\sigma_A = \frac{\Delta A}{\sqrt{N}}, \tag{3.3.1}$$

where ΔA is the population standard deviation and N is the number of trajectories.

Typically, for good convergence, we require $\frac{\sigma_A}{\langle A \rangle} \ll 1$, where $\langle A \rangle$ is the correct mean of the operator $\hat{A}$. This then implies that $N \gg \frac{\Delta A}{\langle A \rangle}$.

An error graph for the specific example we will consider in sub-section (2.4.3) is shown in Figure (2). The plot shows the statistical error (dashed red line), calculated from equation (3.3.1), and the absolute error (solid blue line), which is the average difference between the numerical and analytical result, varying with the number of trajectories. The absolute error fluctuates quite heavily but looks to level off around 1000 trajectories. The statistical error also has significant diminishing returns past 1000 trajectories. It is extremely computationally expensive to run simulations with a high number of trajectories so a balance needs to be struck between accuracy and computation time. Thus, in this case, we chose to use 2000 trajectories, which should provide less than a 1% error at worst.

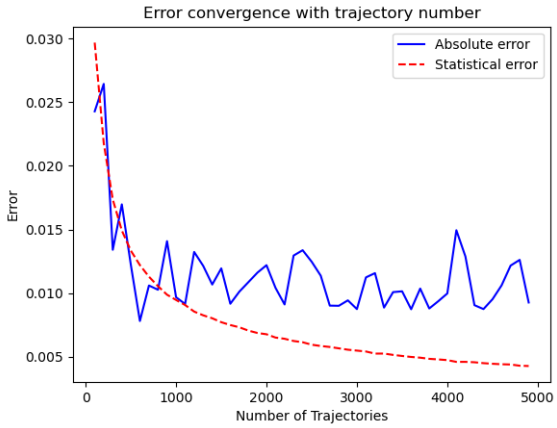

Figure 2: A plot showing how the statistical error (dashed red line), calculated from (3.3.1), and the absolute error (solid blue line), which is the average difference between the numerical and analytical result, vary with the number of trajectories.

3.4. Physical interpretation

As mentioned in the introduction to this section, the quantum trajectories method provides a simple physical interpretation for the effect the environment has on our system. Consider a two-level system, where we drive the ground state, $|g\rangle$, and excited state, $|e\rangle$, with effective Rabi frequency Ω and detuning ν. The system will undergo coherent dynamics interrupted

by spontaneous jumps to the ground or excited state via the action of jump operators such as $c_m = \sqrt{\Gamma_m}\,|g\rangle\langle e|$ or $c_m^\dagger = \sqrt{\Gamma_m}\,|e\rangle\langle g|$. If the photon can be emitted omnidirectionally, then the different directions would correspond to different jump operators. The master equation can then be interpreted as a stochastic average over all possible times a jump could occur for all possible channels [17, p; 92].

Connecting to experiment, if we could perform perfect measurements of our system, a photon emitted at time t would tell us that the system must have been projected into its ground state. Likewise, no observable photon tells us that the system is evolving under the effective Hamiltonian, H_{eff}.

3.5. Higher-order methods

One disadvantage to the method outlined in Sub-section (3.2) is that it is only first-order in the time-step. This can be marginally improved by expanding to a higher-order, for example $\left|\psi^{(1)}(t+\delta t)\right\rangle (1 - iH_{\text{eff}}\delta t - \frac{H_{\text{eff}}}{2}t^2 + ...)\,|\psi(t)\rangle$, or even perform the calculation exactly, i.e $\left|\psi^{(1)}(t+\delta t) = e^{-iH_{\text{eff}}t}\,|\psi(t)\rangle\right\rangle$. However, it is more interesting to note that the method has a systematic error. In reality, the quantum jumps performed by the system would be instantaneous, but in the algorithm the jumps take a time-step δt. This leads to a slight underestimation in the number of jumps that occur in a given time. A revised scheme was created by Dum *et al.*, which involves taking the continuous limit $\delta t \to 0$ [19]. Instead of generating a random number to compare with a probability δp, as was done in step 4 of the first-order method, we use the random number to numerically solve for the time at which the next jump occurs, t_1, given the previous jump, or the start of the evolution, began at t_0, via the following equation [17, p; 94]

$$||\exp(-iH_{\text{eff}}t_1)\,|\psi(t_0)\rangle|| = r, \tag{3.5.1}$$

where the double vertical bracers represents the norm of the state.

Despite being a more accurate method, the first-order method is both more convenient for ensemble averages and less computationally expensive. Since we are most interested in long-time ensemble averages, going forward we will use the first order method exclusively.

3.6. Illustrative examples

We now look to apply the quantum trajectory technique to the two illustrative examples discussed at the end of Section (2), namely the spin-boson model in both the simplified case, without tunnelling, and more general case, with tunnelling.

3.6.1 Spin-boson model without tunnelling

Using the optical master equation in the rotating frame, as stated in equation (2.4.27), and the general form of the Lindbladian master equation, as in equation (3.0.1), we can read off the form of the effective Hamiltonian, using equation (3.0.3), as

$$H_{\text{eff}} = \frac{\nu'}{2}\sigma_z + \frac{\Omega}{2}\sigma_x - i\Gamma(\epsilon)N(\epsilon)\sigma_-\sigma_+ - i\Gamma(\epsilon)(1+N(\epsilon))\sigma_+\sigma_-. \tag{3.6.1}$$

Using this equation and the algorithm outline in Sub-section (3.2) we propagate an initial state forward in time. Two sample trajectories are shown in the right image of Figure (3) for the

specific case with detuning $\nu' = 0$, Rabi frequency $\Omega = 1\text{meV}$, rate $\Gamma = \frac{\Omega}{6}$, to satisfy the secular approximation, $\epsilon = 1\text{eV}$, a typical optical transition frequency, and temperature $T = 298\text{K}$, i.e room temperature. The trajectories undergo Rabi oscillations which are intermittently broken by quantum jumps at random points. A jump to the ground state corresponds to stimulated or spontaneous emission, whereas a jump to the excited state corresponds to absorption.

We can now repeat this for multiple sample trajectories and take the stochastic average to determine the ensemble behaviour. This is shown in the left image of Figure (3). For comparison, we show the exact solution which matches the quantum jump solution within its error for most of the evolution. Beyond $t\Omega = 30$ the two begin to diverge suggesting we need more than 2000 trajectories for reliable prediction here. In the long time limit, the average population of the excited states tends to slightly less than 0.5, as can be seen by substituting our parameters into equation (2.4.29), which physically we interpret as the decay due to both spontaneous and stimulated emission being approximately equal to the pumping from absorption.

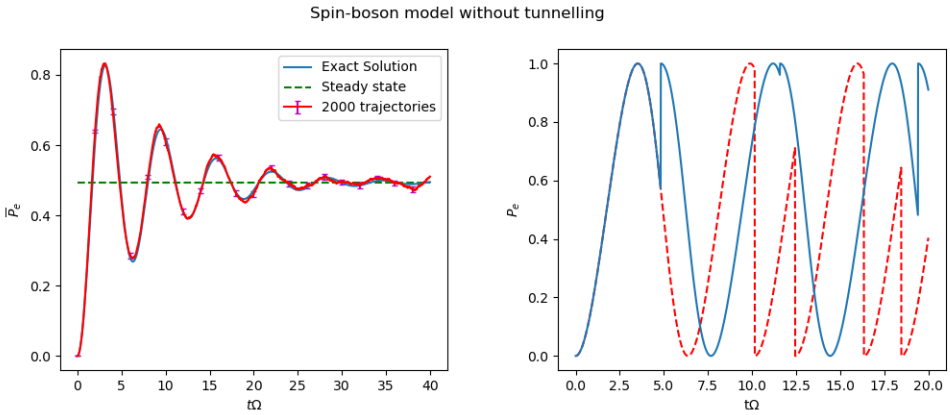

Figure 3: Illustrative example of quantum trajectories for the spin-boson model without tunnelling. Right: probability to find the atom in the excited state, for two random sample trajectories starting in the ground state. Left: population of the excited state averaged over 2000 trajectories (red line), compared with the exact solution found from direct integration of the master equation (blue line) using the Python QuTiP package [20]. The steady state solution is also shown (dashed green line). In both cases we choose detuning $\nu' = 0$, Rabi frequency $\Omega = 1\text{meV}$, rate $\Gamma = \frac{\Omega}{6}$, optical transition frequency $\epsilon = 1\text{eV}$ and temperature $T = 298\text{K}$.

3.6.2 Spin-boson model with tunnelling

In an analogous fashion to the analysis of the case without tunnelling we use the specific form of the master equation in Lindblad form, as written in equation (2.4.33), to read off the effective Hamiltonian

$$\begin{aligned} H_{\text{eff}} = H_S &- i\frac{\Gamma_0}{2}P_0^2 \\ &- i\frac{\Gamma(\eta)}{2}(1 + N(\eta))P_\eta^\dagger P_\eta \\ &- i\frac{\Gamma(\eta)}{2}N(\eta)P_\eta P_\eta^\dagger. \end{aligned} \tag{3.6.2}$$

The H_{LS} term has been ignored as it is usually negligible. We require a specific form for Γ_0 and $\Gamma(\eta)$, which from equations (2.4.36) and (2.4.37) requires specifying a form for $J(\epsilon)$. The

simplest choice is an Ohmic form, i.e $J(\epsilon) = \alpha\epsilon$, where α is the coupling strength. We now re-write the expressions for the rates explicitly as

$$\begin{aligned}\Gamma_0 &= 2\pi \lim_{\epsilon\to 0} \alpha\epsilon(1 + 2N(\epsilon)) \\ &\approx 2\pi \lim_{\epsilon\to 0} \alpha\epsilon \left(1 + \frac{2k_BT}{\epsilon}\right) \\ &= 4\pi\alpha k_BT,\end{aligned} \tag{3.6.3}$$

where we have used the fact that

$$N(\epsilon) = \frac{1}{e^{\frac{\epsilon}{k_BT}} - 1} \approx \frac{k_BT}{\epsilon}, \tag{3.6.4}$$

for small values of ϵ. Similarly,

$$\Gamma(\eta) = 2\pi J(\eta) = 2\pi\alpha\eta. \tag{3.6.5}$$

Choosing similar parameters to our analysis of the optical Bloch equations, we set the detuning $\nu = 0$, then η becomes equivalent to the tunnelling coefficient Δ which is set to 1meV as before. The optical transition frequency is again $\epsilon = 1$eV and $\Gamma = \frac{\Delta}{6}$, which fulfills the condition $\Gamma \ll \eta$ as required for the secular approximation. Equation (3.6.5) then implies that $\alpha = \frac{1}{12\pi}$.

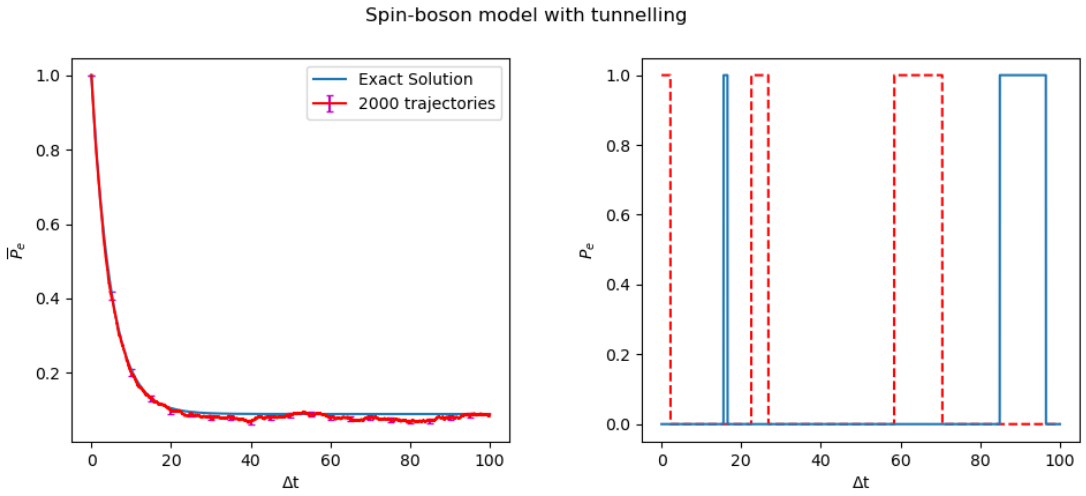

Figure 4: Illustrative example of quantum trajectories for the spin-boson model with tunnelling, working in the energy eigenbasis. Right: population of the excited state for two random sample trajectories propagating in time, one starting in the ground state (solid blue line) and one in the excited state (dashed red line). Left: population of the excited state averaged over 2000 trajectories compared with the exact solution calculated from direct integration of the master equation using the Python QuTiP package [20]. In both cases we choose detuning $\nu = 0$, tunnelling Δ = 1meV, optical transition frequency $\epsilon = 1$eV, coupling strength $\alpha = \frac{1}{12\pi}$ and temperature $T = 5000$K.

Since we chose to work in the energy eigenbasis rather than the z-basis, we no longer get oscillations like those of Figure (3). Instead our initial state is not affected by propagation under the effective Hamiltonian, it remains as is until a quantum jump occurs, at which time it moves to the other eigenstate. Two random sample trajectories, plotting the excited population with time,

are shown in the right image of Figure (4), one starting in the ground state (solid blue line) and the other starting in the excited state (dashed red line).

Again, averaging over 2000 trajectories we obtain the ensemble behaviour, shown in the left image of Figure (4). For the most part this agrees with the exact solution within it's error range. We see in the long time limit, our bosonic bath thermalises the system.

4. Conclusion

In conclusion, We began the project by first considering closed quantum systems and recognising that a more sophisticated framework was needed to treat real-world quantum systems. This lead to the introduction of various mathematical tools such as the density operator, interaction picture and master equation. We showed the general procedure for deriving such master equations, specifically in Linbladian form, and did so in the case of the spin-boson model: a two-level system coupled to a bath of bosonic oscillators, in the case of both a zero and finite tunnelling coefficient. The main focus was on the quantum trajectories technique which was a numerical method to solve for the dynamics of a system by stochastically averaging individual trajectories. We demonstrated this was equivalent to the master equation formulation and then outlined the algorithm for a first-order method in detail, as well as mentioning potential higher-order methods. Additionally, we analysed the errors in this method and highlighted the useful physical insight it provides. Finally, we demonstrated the algorithm in action for the two illustrative examples mentioned.

There are many interesting extensions that could be made to this work. For example, considering the effects of varying the coupling strength or temperature. Switching to a time-dependent Hamiltonian is also another potential avenue of exploration. Additionally, it would be interesting to look at the entropy flow. Particularly on individual trajectories where, due to the quantum jumps, it is likely discontinuous but would be conserved in the ensemble average.

5. Length and date

The number of words in this document is 4956
This document was submitted on 08/01/21 at 17:30

References

[1] J. Von Neumann, "Wahrscheinlichkeitstheoretischer aufbau der quantenmechanik," *Nachrichten von der Gesellschaft der Wissenschaften zu Göttingen, Mathematisch-Physikalische Klasse*, vol. 1927, pp. 245–272, 1927.

[2] D. A. Lidar, "Lecture notes on the theory of open quantum systems," *arXiv preprint arXiv:1902.00967*, 2019.

[3] K. Mølmer, Y. Castin, and J. Dalibard, "Monte carlo wave-function method in quantum optics," *JOSA B*, vol. 10, no. 3, pp. 524–538, 1993.

[4] D. J. Griffiths and D. F. Schroeter, *Introduction to quantum mechanics*. Cambridge University Press, 2018.

[5] R. Shankar, *Principles of quantum mechanics*. Springer Science & Business Media, 2012.

[6] G. Schaller, *Open quantum systems far from equilibrium*, vol. 881. Springer, 2014.

[7] M. A. Nielsen and I. Chuang, "Quantum computation and quantum information," 2002.

[8] H.-P. Breuer, F. Petruccione, *et al.*, *The theory of open quantum systems*. Oxford University Press on Demand, 2002.

[9] J. J. Sakurai and E. D. Commins, "Modern quantum mechanics, revised edition," 1995.

[10] E. W. Weinstein, "Matrix trace." `https://mathworld.wolfram.com/MatrixTrace.html`. Accessed: 09-12-2020.

[11] D. Manzano, "A short introduction to the lindblad master equation," *AIP Advances*, vol. 10, no. 2, p. 025106, 2020.

[12] J. F. Haase, A. Smirne, J. Kołodyński, R. Demkowicz-Dobrzański, and S. F. Huelga, "Fundamental limits to frequency estimation: a comprehensive microscopic perspective," *New Journal of Physics*, vol. 20, no. 5, p. 053009, 2018.

[13] R. C. Hilborn, "Einstein coefficients, cross sections, f values, dipole moments, and all that," *American Journal of Physics*, vol. 50, no. 11, pp. 982–986, 1982.

[14] P. L. Knight and P. W. Milonni, "The rabi frequency in optical spectra," *Physics Reports*, vol. 66, no. 2, pp. 21–107, 1980.

[15] C. Fleming, N. Cummings, C. Anastopoulos, and B. Hu, "The rotating-wave approximation: consistency and applicability from an open quantum system analysis," *Journal of Physics A: Mathematical and Theoretical*, vol. 43, no. 40, p. 405304, 2010.

[16] F. Riehle, *Frequency standards: basics and applications*. John Wiley & Sons, 2006.

[17] A. J. Daley, "Quantum trajectories and open many-body quantum systems," *Advances in Physics*, vol. 63, no. 2, pp. 77–149, 2014.

[18] D. Xu and J. Cao, "Non-canonical distribution and non-equilibrium transport beyond weak system-bath coupling regime: A polaron transformation approach," *Frontiers of Physics*, vol. 11, no. 4, p. 110308, 2016.

[19] R. Dum, A. Parkins, P. Zoller, and C. Gardiner, "Monte carlo simulation of master equations in quantum optics for vacuum, thermal, and squeezed reservoirs," *Physical Review A*, vol. 46, no. 7, p. 4382, 1992.

[20] J. R. Johansson, P. D. Nation, and F. Nori, "Qutip: An open-source python framework for the dynamics of open quantum systems," *Computer Physics Communications*, vol. 183, no. 8, pp. 1760–1772, 2012.